

# Generation and spectral engineering of pulsed polarization entangled states

Yoon-Ho Kim\* and Warren P. Grice

Center for Engineering Science Advanced Research  
Computer Science and Mathematics Division  
Oak Ridge National Laboratory  
Oak Ridge, TN 37831-6355

## ABSTRACT

The quantum state of the photon pair generated from type-II spontaneous parametric down-conversion pumped by a ultrafast laser pulse exhibits strong decoherence in its polarization entanglement, an effect which can be attributed to the clock effect of the pump pulse or, equivalently, to distinguishing spectral information in the two-photon state. Here, we discuss novel spectral engineering techniques to eliminate these detrimental decoherence effects. In addition, spectral engineering also provides a means for generating polarization entangled states with novel spectral characteristics: the frequency-correlated state and the frequency-uncorrelated state. Such states may find usefulness in experimental quantum information science and quantum metrology applications.

**Keywords:** Quantum entanglement, spontaneous parametric down conversion, joint spectrum

## 1. INTRODUCTION

Entangled quantum states,<sup>1</sup> once discussed mainly in the context of the philosophical and foundational problems in quantum mechanics, are now at the heart of the rapidly developing field of quantum information science.<sup>2</sup> In addition, many researchers are hoping to exploit the unique features of the entangled states in order to surpass the “classical limit” in applications such as quantum lithography,<sup>3</sup> the quantum optical gyroscope,<sup>4</sup> quantum clock synchronization and positioning,<sup>5</sup> etc.

A particularly convenient and reliable source of entangled particles is the process of type-II spontaneous parametric down-conversion (SPDC),<sup>6–10</sup> in which an incident pump photon is split into two orthogonally polarized lower energy daughter photons (usually called signal and idler) inside a crystal with a  $\chi^{(2)}$  nonlinearity, such as BBO, LBO, KTP, etc. Initially, the photon pairs are entangled in energy, time, and momentum due to the energy and momentum conservation conditions (the phase matching condition) that govern the process. In addition, polarization entanglement may be obtained as a result of specific local operations on the photon pair.<sup>7–10</sup> An optical process such as this has the advantage that the photons, once generated, interact rather weakly with the environment, thus making it possible to maintain entanglement for relatively long periods of time.

In this paper, we discuss efficient generation schemes for pulsed two-photon polarization entangled states. Pulsed polarization entangled states are an essential ingredient in many experiments in quantum optics. They are useful, for example, as building blocks for entangled states of three or more photons.<sup>11</sup> (In general, the SPDC process only results in two-photon entanglement.) Pulsed two-photon entangled states are also useful in practical quantum cryptography systems, since the well-known arrival times permit gated detection. We also discuss how to engineer the spectral properties of the two-photon state produced in the type-II SPDC process pumped by a ultrafast laser pulse (ultrafast type-II SPDC) to generate two-photon entangled states with novel spectral properties: frequency-correlated and frequency-uncorrelated states. Such novel frequency-engineered two-photon or multi-photon states have recently shown to be useful for quantum metrology applications.<sup>5</sup>

We begin in section 2 with a discussion of the limitations of the state-of-the-art techniques for the generation of polarization-entangled photon pairs. We then, in section 3, discuss specific spectral engineering techniques.

---

\*kimy@ornl.gov; phone: 1 865 241 0912; fax: 1 865 241 0381

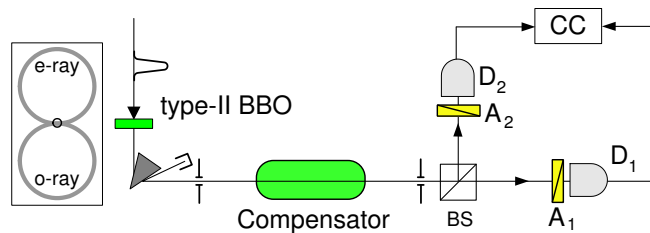


**Figure 1.** Typical experimental setup for preparing a Bell-state using collinear type-II SPDC. The compensator is used to compensate the longitudinal walk-off between the e-ray and the o-ray of the crystal.  $A_1$  and  $A_2$  are the polarization analyzers and  $D_1$  and  $D_2$  are the single-photon detectors.  $CC$  is the coincidence circuit.

## 2. ENTANGLEMENT IN TYPE-II SPDC

Let us briefly review one of the standard techniques for generating polarization entangled two-photon states (Bell-states\*) via type-II SPDC.<sup>8-10</sup> A typical experimental setup is shown in Fig. 1. A type-II nonlinear crystal is pumped with a UV laser beam and the orthogonally polarized signal (e-ray; vertically polarized) and idler (o-ray; horizontally polarized) photons, which are in the near infrared, travel collinearly with the pump. After passing through a prism sequence to remove the pump, the signal-idler photon pair is passed through a compensator (a quartz delay line which introduces the relative delay  $\tau$  between the e-ray and the o-ray of the crystal) before the beamsplitter (BS) splits the SPDC beam into two spatial modes 1 and 2. A polarization analyzer and a single-photon detector are placed at each output port of the beamsplitter for polarization correlation measurements. In this case, the two quantum mechanical amplitudes in which both photons end up at the same detector are not registered since only coincidence events are considered. That is, a state post-selection has been made.<sup>8,9,12</sup> A noncollinear type-II SPDC method developed later resolved this state post-selection problem and is usually regarded as the “standard” method for generating polarization entangled photon pairs.<sup>10</sup>

Both the collinear and noncollinear type-II SPDC methods work very well for the generation of polarization entangled photon pairs when the UV pump laser is continuous wave (cw). In this case, however, there is no information available regarding the photons’ arrival times at the detectors. Such timing information can be quite useful in certain applications, as discussed in section 1. If the UV pump has the form of an ultrafast optical pulse ( $\approx 100$  fsec), then the photon pair arrival times can be known within a time interval on the order of the pump pulse duration. However, it has been theoretically and experimentally shown that, in general, type-II SPDC suffers the loss of quantum interference if the pump is delivered in the form of an ultrafast pulse.<sup>13,14</sup>

We will first briefly review the theoretical treatment of the ultrafast type-II SPDC process and discuss the physical mechanism of the loss of quantum interference (or decoherence). With this understanding in hand, we then discuss in the subsequent sections three methods for eliminating this decoherence through spectral engineering of the two-photon state.

From first-order perturbation theory, the quantum state of type-II SPDC may be expressed as<sup>9,13</sup>

$$|\psi\rangle = -\frac{i}{\hbar} \int_{-\infty}^{\infty} dt \mathcal{H}|0\rangle, \quad (1)$$

where

$$\mathcal{H} = \epsilon_0 \int d^3\vec{r} \chi^{(2)} E_p(z, t) E_o^{(-)} E_e^{(-)}$$

---

\*There are four orthonormal Bell-states:

$$|\psi^{(\pm)}\rangle = \frac{1}{\sqrt{2}}(|H\rangle_1|V\rangle_2 \pm |V\rangle_1|H\rangle_2) \quad \text{and} \quad |\phi^{(\pm)}\rangle = \frac{1}{\sqrt{2}}(|H\rangle_1|H\rangle_2 \pm |V\rangle_1|V\rangle_2).$$

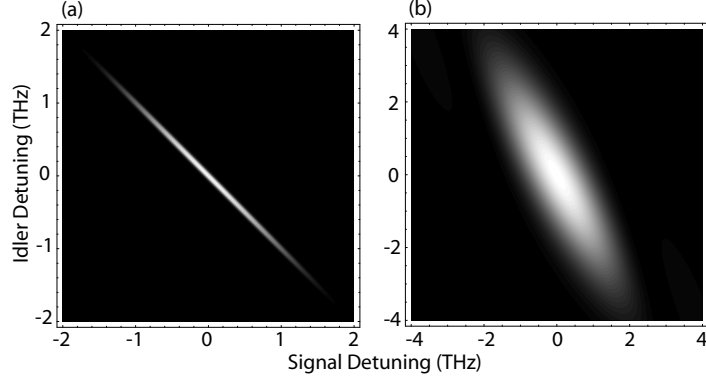


**Figure 2.** (a) Calculated joint spectrum for cw-pumped type-II SPDC. The joint spectrum is symmetric. (b) Calculated joint spectrum for ultrafast type-II SPDC. The joint spectrum is now asymmetric. For both cases, the signal and the idler photons are frequency anti-correlated.

is the Hamiltonian governing the SPDC process. The pump electric field,  $E_p(z, t)$ , is considered classical and is assumed to have a Gaussian shape in the direction of propagation. The operator  $E_o^{(-)}$  ( $E_e^{(-)}$ ) is the negative frequency part of the quantized electric field of o-polarized (e-polarized) photon inside the crystal. Integrating over the length of the crystal,  $L$ , Eq. (1) can be written as

$$|\psi\rangle = C \iint d\omega_e d\omega_o \operatorname{sinc}\left(\frac{\Delta L}{2}\right) \mathcal{E}_p(\omega_e + \omega_o) a^\dagger(\omega_e) a^\dagger(\omega_o) |0\rangle, \quad (2)$$

where  $C$  is a constant and  $\Delta \equiv k_p(\omega_p) - k_o(\omega_o) - k_e(\omega_e)$ . The pump pulse is described by  $\mathcal{E}_p(\omega_e + \omega_o) = \exp\{-(\omega_e + \omega_o - \Omega_p)^2 / \sigma_p^2\}$ , where  $\sigma_p$  and  $\Omega_p$  are the bandwidth and the central frequency of the pump pulse, respectively.  $a^\dagger(\omega_e)$ , for example, is the creation operator for the e-polarized photon of frequency  $\omega_e$ .

The spectral properties of the two-photon state type-II SPDC are best illustrated in plots of the two-photon joint spectrum, which can be regarded as a probability distribution for the photon frequencies. Recall that the two-photon state  $|\psi\rangle$  given in Eq. (2) contains the phase mismatch term  $\operatorname{sinc}(\Delta L/2)$  and the pump envelope term  $\mathcal{E}_p(\omega_e + \omega_o)$ . The joint spectrum function is simply the square modulus of the product of these two terms:

$$S(\omega_e, \omega_o) = |\operatorname{sinc}(\Delta L/2) \mathcal{E}_p(\omega_e + \omega_o)|^2.$$

Fig. 2 shows examples of two-photon joint spectrum for cw- and ultrafast-pumped type-II SPDC. For the cw case, the pump wavelength is 351.1 nm and the SPDC is centered at 702.2 nm, which is typical. It is clear that the joint spectrum is symmetric. For the ultrafast case, typical pumping conditions are 400 nm centered 100 fsec FWHM ultrafast pulse. The SPDC photons are centered at 800 nm. It is quite clear that the joint spectrum is now asymmetric.

The symmetry of the joint spectrum function  $S(\omega_e, \omega_o)$  has significant effects on the quality of the polarization entanglement. The general form of the quantum state  $|\psi\rangle$  after the beamsplitter takes the form

$$|\psi\rangle = C \iint d\omega_e d\omega_o S(\omega_e, \omega_o) a_1^\dagger(\omega_e) a_2^\dagger(\omega_o) |0\rangle - C \iint d\omega_e d\omega_o S(\omega_o, \omega_e) a_1^\dagger(\omega_o) a_2^\dagger(\omega_e) |0\rangle, \quad (3)$$

when the longitudinal walk-off between the e-ray and o-ray inside the crystal is properly compensated by the compensator shown in Fig. 1.  $a_1^\dagger(\omega_e)$ , for example, is the creation operator for the e-polarized photon of frequency  $\omega_e$  at detector 1.

Therefore, if the joint spectrum is symmetric,  $S(\omega_e, \omega_o) = S(\omega_o, \omega_e)$ , the spectral integral part simply factors out and the above equation can be written as (after proper normalization)  $|\psi^{(-)}\rangle = \frac{1}{\sqrt{2}}(|e\rangle_1 |o\rangle_2 - |o\rangle_1 |e\rangle_2)$ ,

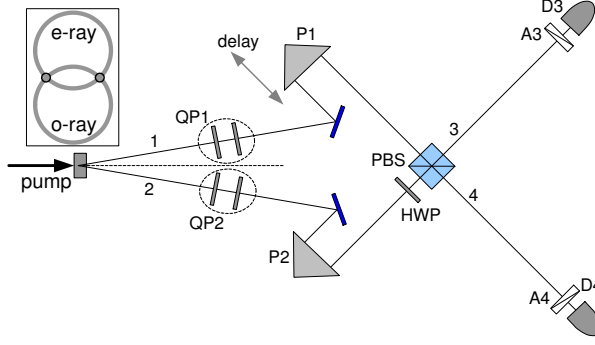


**Figure 3.** Schematic for interferometric method of producing pulsed Bell-states from ultrafast type-II SPDC. Non-collinear type-II SPDC is used to prepare the state described in Eq. 4. QP1 and QP2 are thin quartz plates for phase adjustment and HWP is the  $\lambda/2$  plate oriented at  $45^\circ$ .

which is a pure polarization entangled two-photon state (Bell-state). Indeed, this is the case of cw-pumped type-II SPDC and Bell-states with high degree of entanglement is routinely reported in literature.<sup>8–10</sup> This factorization, however, does not work if the joint spectrum function is not symmetric as shown in Fig. 2(b). This has the effect of reducing the the quality of quantum interference (the degree of polarization entanglement) and has been confirmed experimentally.<sup>13, 14</sup>

As mentioned in section 1, pulsed Bell-states have many more potential applications than cw Bell-states since the arrival time of the entangled photon pair can be known within several hundreds of femtoseconds. As we have shown so far, ultrafast type-II SPDC is not able to provide high degree of polarization entanglement due to asymmetric joint spectrum. It is however possible to enhance the entanglement in two ways: (i) through the use of narrowband spectral filters to select only the symmetric or overlapping part of the joint spectrum functions and/or (ii) by decreasing the thickness of the crystal. The idea here is that the increased overall bandwidth of the SPDC (due to the reduction in the crystal thickness) also increases the relative overlap or the symmetric areas. Although entanglement can be increased in these ways, the above methods severely reduce the number of available entangled photon pairs.

### 3. SPECTRAL ENGINEERING

In section 2, we have shown that current methods of generating pulsed Bell-states lack the necessary efficiency and versatility for use in many quantum applications. In this section, we discuss novel methods of generating pulsed Bell-states in ultrafast type-II SPDC without using narrowband spectral filtering.

#### 3.1. Interferometric method

In this section, we discuss a novel interferometric method of producing pulsed Bell-state from ultrafast type-II SPDC without relying on narrowband spectral filtering. Consider the experimental arrangement shown in Fig. 3. As in Ref. 10, we restrict our attention to non-collinear SPDC photons found in the intersections of the cones made by the e- and the o-rays exiting the crystal. The quantum state of the photon pair found in the mode 1 and 2 can be written as

$$|\psi\rangle = C \iint d\omega_e d\omega_o S(\omega_e, \omega_o) a_1^\dagger(\omega_e) a_2^\dagger(\omega_o) |0\rangle + C \iint d\omega_e d\omega_o S(\omega_o, \omega_e) a_1^\dagger(\omega_o) a_2^\dagger(\omega_e) |0\rangle. \quad (4)$$

As we discussed in section 2, the joint spectrum function is symmetric for the cw type-II SPDC but asymmetric for the ultrafast type-II SPDC. Therefore, the spectral part of the wavefunction does not factor out in general. The density matrix of the polarization variable of the two-photon state alone can then be written as

$$\rho_{mix} = \frac{1}{2} (|H_1\rangle|V_2\rangle\langle V_2| + |H_1\rangle|H_2\rangle\langle H_2| + |V_1\rangle|H_2\rangle\langle H_2| + |V_1\rangle|V_2\rangle\langle V_2|),$$

which is a mixed state. As we shall show now, it is nevertheless possible to use rather simple interferometric technique to make two joint spectrum functions equal so that they factor out from the wavefunction, making the polarization part of the wavefunction entangled. We may call this process “filtering-free entanglement concentration”.<sup>15</sup>

Let us now consider how the initial wavefunction Eq. (4) is transformed by a set of linear optical elements (HWP-PBS). The original wavefunction contains two polarization amplitudes,  $|V\rangle_1|H\rangle_2$  and  $|H\rangle_1|V\rangle_2$ , which are associated with their own joint spectrum functions. The HWP-PBS set transforms these two amplitudes into  $|V\rangle_3|V\rangle_4$  and  $|H\rangle_3|H\rangle_4$ . The full wavefunction can then be written as

$$|\psi\rangle = C \iint d\omega_e d\omega_o S(\omega_e, \omega_o) a_{V3}^\dagger(\omega_e) a_{V4}^\dagger(\omega_o) |0\rangle + C \iint d\omega_e d\omega_o S(\omega_e, \omega_o) a_{H3}^\dagger(\omega_e) a_{H4}^\dagger(\omega_o) |0\rangle, \quad (5)$$

where  $a_{V3}^\dagger(\omega_e)$ , for example, is the creation operator for the vertically polarized photon of frequency  $\omega_e$  which originally belonged to the e-ray of the crystal. Note that the e-ray (which is either vertically or horizontally polarized) is always detected by detector 3 and the o-ray is always detected by detector 4. This removes the intrinsic timing information that had been present in the wavefunction which was due to the group velocity difference between the e-ray and the o-ray in the nonlinear crystal. Since the joint spectrum functions in each amplitudes in Eq. (5) has the same form, they can be integrated out, leaving only the polarization part of the wavefunction. The polarization part of the wavefunction can then be written as

$$|\psi\rangle = |\phi^{(+)}\rangle = \frac{1}{\sqrt{2}}(|V\rangle_3|V\rangle_4 + |H\rangle_3|H\rangle_4), \quad (6)$$

which is pure entangled state. By using a set of  $\lambda/2$  plates, the above state can then be transformed to other forms of Bell-states easily. Note also that the interferometric technique described in this section is quite universal in the sense that the emerging polarization entangled state is not affected by spectral filtering, thickness of the nonlinear crystal, and the choice of pump source (cw or ultrafast).

### 3.2. Symmetrization of the joint spectrum

In section 3.1, we discussed how a set of simple linear optical elements can be used to produce an efficient source of pulsed Bell-states. In this method, the shape of the joint spectrum function does not change. In this section, we discuss how one can generate pulsed Bell-state efficiently by directly modifying the joint spectrum function.

As we have learned in section 2, ultrafast type-II SPDC suffers decoherence in polarization entanglement due to the asymmetric joint spectrum function. Our approach here is to symmetrize the joint spectrum function via a proper choice of crystal and pump parameters. This approach was first described by Keller and Rubin in time domain in Ref. 11 and the connection to the spectral domain was identified later by Grice *et al.*<sup>16</sup> and Kim and Grice.<sup>17</sup> Here, we briefly describe the time domain picture by Keller and Rubin and then make a connection to the spectral domain as done in Ref. 17.

Let us now consider the experimental setup shown in Fig. 1. The electric field operators at the detectors are

$$\begin{aligned} E_1^{(+)} &= \frac{1}{\sqrt{2}} \int d\omega' \{ \cos \theta_1 e^{-i\omega'(t_1+\tau)} a_e(\omega') - \sin \theta_1 e^{-i\omega' t_1} a_o(\omega') \}, \\ E_2^{(+)} &= \frac{i}{\sqrt{2}} \int d\omega' \{ \cos \theta_2 e^{-i\omega'(t_2+\tau)} a_e(\omega') + \sin \theta_2 e^{-i\omega' t_2} a_o(\omega') \}, \end{aligned}$$

where  $\theta_1$  and  $\theta_2$  are the angles of the polarization analyzers  $A_1$  and  $A_2$  and  $\tau$  is the delay introduced by the compensator. Here we have assumed no spectral filtering before detection. The coincidence count rate at the detectors is proportional to

$$\begin{aligned} R_c &\propto \int dt_1 \int dt_2 |\langle 0 | E_2^{(+)} E_1^{(+)} | \psi \rangle|^2 \\ &= \int dt_+ \int dt_- |\mathcal{A}(t_+, t_-)|^2, \end{aligned} \quad (7)$$

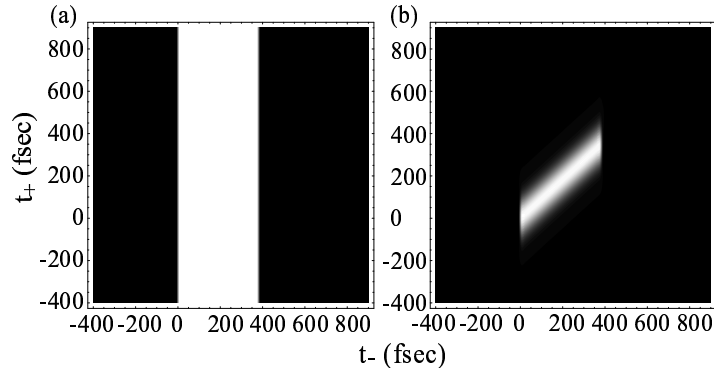


**Figure 4.** Calculated two-photon wavefunction  $\Pi(t_+, t_-)$  for type-II SPDC. (a) For a cw-pumped case. The two-photon wavefunction is independent of  $t_+$  and has the rectangular shape in  $t_-$ . (b) For a 100 fsec pump pulse. It is strongly asymmetric. See Fig. 2 for corresponding joint spectrum functions.

where  $t_+ = (t_1 + t_2)/2$ ,  $t_- = t_1 - t_2$ , and  $|\psi\rangle$  is shown in Eq. (2).

The two-photon amplitude  $\mathcal{A}(t_+, t_-)$  has the form

$$\mathcal{A}(t_+, t_-) = \cos \theta_1 \sin \theta_2 \Pi(t_+, t_- + \tau) - \sin \theta_1 \cos \theta_2 \Pi(t_+, -t_- + \tau), \quad (8)$$

where

$$\Pi(t_+, t_-) = \begin{cases} e^{-i\Omega_p t_+} e^{-\sigma_p^2 \{t_+ - [D_+/D]t_-\}^2} & \text{for } 0 < t_- < DL \\ 0 & \text{otherwise.} \end{cases} \quad (9)$$

The parameters  $D_+$  and  $D$  are defined to be

$$D_+ = \frac{1}{2} \left( \frac{1}{u_o(\Omega_o)} + \frac{1}{u_e(\Omega_e)} \right) - \frac{1}{u_p(\Omega_p)},$$

$$D = \frac{1}{u_o(\Omega_o)} - \frac{1}{u_e(\Omega_e)},$$

where, for example,  $u_o(\Omega_o)$  is the group velocity of o-polarized photon of frequency  $\Omega_o$  in the crystal.

It is clear from Eqs. (7) and (8) that the degree of quantum interference is directly related to the amount of overlap between the two two-photon wavefunctions  $\Pi(t_+, t_- + \tau)$  and  $\Pi(t_+, -t_- + \tau)$ . Figure 4 shows calculated two-photon wavefunctions for type-II SPDC in a 2 mm Beta-Barium Borate (BBO) crystal with a central pump wavelength of 400 nm. The two-photon wavefunction for the cw-pumped case is symmetric in  $t_+$  and  $t_-$ . As shown in Fig. 4(a), it has a rectangular shape in the  $t_-$  direction and extends to infinity in the  $t_+$  direction. In the case of ultrafast type-II SPDC, the two-photon wavefunction is strongly asymmetric, see Fig. 4(b). Comparing Fig. 2 and Fig. 4, we can immediately see the correspondence between the time domain picture and the spectral domain picture. In either case, the asymmetry in two-photon wavefunction or joint spectrum function leads to decoherence in polarization entanglement.

How can we then remove this asymmetry? Upon careful inspection of Eq. (9), we find that if  $D_+/D$  is made to vanish,  $\Pi(t_+, t_-)$  becomes symmetric. For a type-II BBO crystal,  $D_+ = 0$  occurs when the central wavelength of the pump pulse is 757 nm and the SPDC is centered at 1.514  $\mu\text{m}$ . The joint spectrum for this case is shown in Fig. 5 for a crystal thickness of 2 mm and a pump bandwidth of 8 nm. Note that the signal and the idler photons have identical spectra. Thus, the photon pair is distinguishable only in the polarizations of the photons, as required for a polarization entangled state.

In this example, this approach has an additional advantage: the entangled photon pairs are emitted with central wavelengths of 1514 nm, which is within the standard fiber communication band. Such pulsed entangled

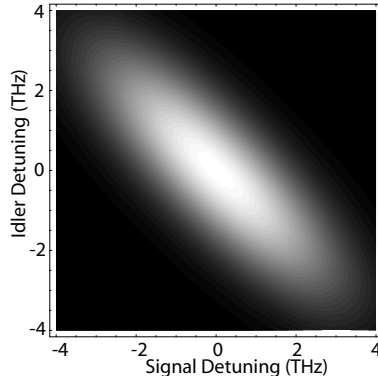


**Figure 5.** Calculated joint spectrum for ultrafast type-II SPDC. The joint spectrum is symmetrized via the spectral engineering technique described in section 3.2.

photons at communication wavelengths may be useful for building practical quantum key distribution systems using commercially installed optical fibers. At this wavelength, of course, single photon detection is more problematic. However, the recent development of single photon counting techniques using InGaAs avalanche photodiodes may soon provide good single photon counters at this wavelength.<sup>18</sup>

### 3.3. Frequency-correlated and -uncorrelated states

The spectral properties of the photon pairs represented in Fig. 2 and Fig. 5 display the tendency of frequency-anticorrelation in the sense that a positive detuning for the signal photon is accompanied by a negative detuning for the idler photon. This effect follows from the energy conservation condition that constrains the SPDC process. In ultrafast type-II SPDC, the anticorrelation is not as strong as in the cw-pumped case due to the broad bandwidth of the pump pulse. However, the general tendency of anti-correlation,  $\omega_s = \omega_p/2 \pm \omega$  and  $\omega_i = \omega_p/2 \mp \omega$  where  $\omega$  is the detuning frequency, is clearly visible in Fig. 2(b) and Fig. 5. This frequency-anticorrelation, however, is not a required feature of the two-photon state. In ultrafast type-II SPDC, two-photon states with novel spectral characteristics – the frequency-correlated state and the frequency-uncorrelated state – may be generated through appropriate choices of the parameters that affect the joint spectrum.

The idea behind two-photon states with novel spectral characteristics is not new. The output characteristics of a beamsplitter and a Mach-Zehnder interferometer for frequency-correlated and frequency-uncorrelated photon pairs are theoretically studied in Ref. 19 with no discussion of how such states might be generated. Frequency-correlated states are also studied in Ref. 20, but the discussions are limited to the generation of frequency-correlated states using quasi-phase matching in a periodically poled crystal. Here, we discuss how frequency-correlated states and frequency-uncorrelated states may be generated via appropriate spectral engineering of the two-photon state in ordinary bulk crystals. Since our main focus is polarization entangled photon pairs with novel spectral characteristics, we restrict our attention to the case in which the two-photon joint spectrum is symmetric, i.e.,  $D_+ = 0$ .

Frequency-correlated state generation via the SPDC process is somewhat counter-intuitive since conservation of energy requires the frequencies of the photon pair to sum to the frequency of the pump photon. This requirement imposes a strong constraint in cw-pumped SPDC, where the pump the pump field is monochromatic. In ultrafast SPDC, however, the pump field has a bandwidth of several terahertz frequency (several nanometers in wavelength) and so the frequencies of the photon pair need only sum to some value within the range of pump frequencies. This extra freedom makes it possible to generate the frequency-correlated state.

Examination of the joint spectrum function  $S(\omega_e, \omega_o)$  suggests that if the bandwidth of the pump envelope  $\mathcal{E}_p(\omega_e + \omega_o)$  is large enough and if the parameters are chosen such that the  $\text{sinc}(\Delta L/2)$  may be approximated

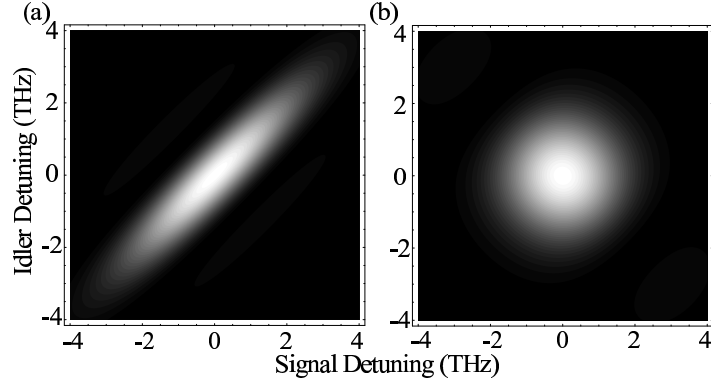


**Figure 6.** Calculated joint spectrum for ultrafast type-II SPDC. The joint spectrum is symmetrized via the spectral engineering technique described in this section.

by the delta function  $\delta(\omega_e - \omega_o)$ , then the two-photon state becomes

$$|\psi\rangle = C \int d\omega \mathcal{E}_p(2\omega) a_e^\dagger(\omega) a_o^\dagger(\omega) |0\rangle, \quad (10)$$

where  $C$  is a constant. Eq. (10) shows the signature of the frequency-correlated state:  $\omega_e = \omega_p/2 \pm \omega$  and  $\omega_o = \omega_p/2 \pm \omega$ . Figure 6(a) shows the calculated joint spectrum function for the frequency-correlated two-photon state. In this example, the pump central wavelength was set to 757 nm in order to satisfy the condition  $D_+ = 0$ , i.e., to assure direct generation of polarization entangled photon pairs. This also has the effect of properly aligning the  $\text{sinc}(\Delta L/2)$  function. The only other requirement is that this function should be narrow enough that it may be approximated as  $\delta(\omega_s - \omega_i)$ . This is achieved by increasing the value of  $L$ , the crystal thickness, since the width of the sinc function is inversely proportional to the crystal length. In Fig. 6(a), it is assumed that a 12 mm thick type-II BBO crystal is pumped by a 20 nm bandwidth ultrafast pulse centered at 757 nm and that, at zero detuning, the wavelengths of the SPDC photons are 1514 nm. The structure of frequency-correlation is clearly illustrated: as the signal detuning increases, the idler detuning is also increased. Such frequency-correlated states have been shown to be useful for certain quantum metrology applications.<sup>5</sup>

By slightly modifying the condition for the generation of the frequency-correlated state, it is possible to generate the frequency-uncorrelated state. By frequency-uncorrelated state, we mean that the frequencies of the two photons are uncorrelated, in the sense that the range of the available frequencies for a particular photon is completely independent of the frequency of its conjugate. As far as the photons are concerned, this means that the spectral properties of one photon are in no way correlated with the spectral properties of the other. The joint spectrum of such a state is shown in Fig. 6(b) where the joint spectrum function is calculated for type-II SPDC in a 5-mm thick BBO crystal pumped by a 10 nm bandwidth ultrafast pump centered at 757 nm. Again, the pump pulse central wavelength is set to 757 nm to ensure symmetry in the joint spectrum. The more general case is discussed in Ref.,<sup>16</sup> where it is also shown that such states are essential in experiments involving interference between photons from different SPDC sources.

#### 4. SUMMARY

The generation of polarization entangled states requires the coherent superposition of two two-photon amplitudes. An additional requirement is that the two amplitudes must be identical in all respects except polarization. This is not the case, in general, when the photon pairs originate in a type-II SPDC process, although only a simple delay is required when the process is pumped by a cw laser. When an ultrafast pumping scheme is employed, however, these techniques typically do not result in the complete restoration of quantum interference. Some improvement is seen with (i) thin nonlinear crystals and/or (ii) narrow spectral filters before the detectors. Unfortunately, both of these techniques result in greatly reduced count rates. By engineering the two-photon

state of ultrafast type-II SPDC in time or in frequency, it is possible to recover the quantum interference without discarding any photon pairs. In addition, spectral engineering holds the promise of two-photon states with novel spectral properties which have not been available previously.

In the interferometric method, the engineering of the two-photon state is accomplished through a set of simple linear optical elements which changes the mode distribution of the two-photon amplitudes. This results in the complete factorization of the spectral part of the wavefunction, leaving pure polarization entanglement, without modifying the shape of the joint spectrum function. The polarization entanglement generated through this method does not suffer the loss of quantum interference common in ultrafast type-II SPDC and the interferometer can be viewed as a universal Bell-state synthesizer since the quantum interference is independent of the crystal properties, the bandwidth of spectral filters, the bandwidth of the pump laser, and the wavelengths.

A different approach is taken in the second and the third method. Here, the asymmetric joint spectrum function  $S(\omega_e, \omega_o)$  from ultrafast type-II SPDC is symmetrized through careful control of the crystal and pump properties. Such spectrally engineered two-photon states exhibit complete quantum interference with no need for auxiliary interferometric techniques. The spectral engineering techniques may also be employed in the generation of two-photon states with novel spectral characteristics: the frequency-correlated state and the frequency-uncorrelated state. Unlike typical two-photon states from the SPDC process, which exhibit strong frequency-anticorrelation, the frequency-correlated state is characterized by a strong positive frequency correlation, while the frequencies of the two photons are completely uncorrelated in the frequency-uncorrelated state.

The spectral engineering techniques studied in this paper are expected play an important role in generating the pulsed entangled photon pairs essential in applications such as practical quantum cryptography, multi-photon entangled state generation, multi-photon interference experiments, etc. Since the interferometric method allows one to control the decoherence in a stable way,<sup>15, 16</sup> it also facilitates the study of the effects of decoherence in entangled multi-qubit systems. In addition, frequency-correlated discussed in this paper may be useful for certain quantum metrology applications.

## ACKNOWLEDGMENTS

We would like to thank M.V. Chekhova, S.P. Kulik, M.H. Rubin, and Y. Shih for helpful discussions. This research was supported in part by the U.S. Department of Energy, Office of Basic Energy Sciences. The Oak Ridge National Laboratory is managed for the U.S. DOE by UT-Battelle, LLC, under contract No. DE-AC05-00OR22725.

## REFERENCES

1. A. Einstein, B. Podolsky, and N. Rosen, *Phys. Rev.* **47**, 777 (1935); J.S. Bell, *Speakable and unspeakable in quantum mechanics*, Cambridge University Press, New York (1987).
2. A. Steane, *Rep. Prog. Phys.* **61**, 117 (1998); M.A. Nielsen and I.L. Chuang, *Quantum Computation and Quantum Information*, Cambridge University Press, New York (2000).
3. A.N. Boto *et al.*, *Phys. Rev. Lett.* **85**, 2733 (2000); M. D'Angelo, M.V. Chekhova, and Y. Shih, *Phys. Rev. Lett.* **87**, 013602 (2001);
4. J.P. Dowling, *Phys. Rev. A* **57**, 4736 (1998).
5. R. Jozsa *et al.*, *Phys. Rev. Lett.* **85**, 2010 (2000); V. Giovannetti, S. Lloyd, and L. Maccone, *Phys. Rev. A* **65**, 022309 (2002).
6. D.N. Klyshko, *Photons and Nonlinear Optics*, Gordon and Breach, New York (1988).
7. T.E. Kiess *et al.*, *Phys. Rev. Lett.* **71**, 3893 (1993).
8. Y.H. Shih and A.V. Sergienko, *Phys. Lett. A* **186**, 29 (1994); Y.H. Shih and A.V. Sergienko, *Phys. Lett. A* **191**, 201 (1994)
9. M.H. Rubin *et al.*, *Phys. Rev. A* **50**, 5122 (1994).
10. P.G. Kwiat *et al.*, *Phys. Rev. Lett.* **75**, 4337 (1995).
11. T.E. Keller *et al.*, *Phys. Rev. A* **57**, 2076 (1998).

12. L. De Caro and A. Garuccio, Phys. Rev. A **50**, R2803 (1994); S. Popescu, L. Hardy, and M. Zukowski, Phys. Rev. A **56**, R4353 (1997); M. Zukowski *et al.*, Phys. Rev. A **60**, R2614 (1999).
13. T.E. Keller and M.H. Rubin, Phys. Rev. A **56**, 1534 (1997); W.P. Grice and I.A. Walmsley, Phys. Rev. A **56**, 1627 (1997).
14. G. Di Giuseppe *et al.*, Phys. Rev. A **56**, R21 (1997); W.P. Grice *et al.*, Phys. Rev. A **57**, R2289 (1998); Y.-H. Kim *et al.*, Phys. Rev. A **64**, 011801(R) (2001); Y.-H. Kim *et al.*, Phys. Rev. Lett. **86**, 4710 (2001).
15. Y.-H. Kim *et al.*, submitted to Phys. Rev. Lett. (2002).
16. W.P. Grice, A.B. U'Ren, and I.A. Walmsley, Phys. Rev. A **64**, 063815 (2001).
17. Y.-H. Kim and W.P. Grice, to appear in J. Mod. Opt. (2002).
18. A. Lacaita *et al.*, Applied Optics **35**, 2986 (1996); G. Ribordy *et al.*, Applied Optics **37**, 2272 (1998); A. Karlsson *et al.*, IEEE Circuits & Devices, Nov., 34, (1999); P.A. Hiskett *et al.*, Applied Optics **39**, 6818 (2000).
19. R.A. Campos, B.E.A. Saleh, and M.C. Teich, Phys. Rev. A **42**, 4127 (1990).
20. V. Giovannetti *et al.*, Phys. Rev. Lett **88**, 183602 (2002).